Hindawi Publishing Corporation
Journal of Nanomaterials
Volume 2012, Article ID 743236, 7 pages
doi:10.1155/2012/743236

Research Article

Surface Modification of $LiMn_2O_4$ for Lithium Batteries by Nanostructured $LiFePO_4$ Phosphate

B. Sadeghi, R. Sarraf-Mamoory, and H. R. Shahverdi

Department of Materials Engineering, Tarbiat Modares University, P.O. Box 4838-141, Tehran, Iran

Correspondence should be addressed to R. Sarraf-Mamoory, rsarrafm@modares.ac.ir

Received 17 May 2012; Revised 31 August 2012; Accepted 31 August 2012

Academic Editor: Christian Brosseau

$LiMn_2O_4$ spinel cathode materials have been successfully synthesized by solid-state reaction. Surface of these particles was modified by nanostructured $LiFePO_4$ via sol gel dip coating method. Synthesized products were characterized by thermally analyzed thermogravimetric and differential thermal analysis (TG/DTA), X-ray diffraction (XRD), scanning electron microscopy (SEM), transmission electron microscopy (TEM), and energy dispersive X-ray spectroscopy (EDX). The results of electrochemical tests showed that the charge/discharge capacities improved and charge retention of battery enhanced. This improved electrochemical performance is caused by $LiFePO_4$ phosphate layer on surfaces of $LiMn_2O_4$ cathode particles.

1. Introduction

Since the birth of the lithium ion battery in the early 1990s, its development has been very fast and it has been widely applied as power source for a lot of light and high value electronics due to its significant advantages over traditional rechargeable battery systems [1, 2]. Due to its low cost and low toxicity, the spinel $LiMn_2O_4$, the cathode for Li-ion batteries, has been extensively investigated. The spinel $LiMn_2O_4$ has a cubic structure with the space group of Fd3m symmetry in which lithium and manganese ions occupy tetrahedral (8a) sites and octahedral (16d) sites, respectively, within a cubic close packed oxygen array with oxygen ions in 32e sites. Many reports revealed that the spinel $LiMn_2O_4$ offers a potentially attractive alternative to the presently commercialized $LiCoO_2$. However, a key problem prohibiting $LiMn_2O_4$ from commercialization is its severe capacity and cycling performance fading during cycling [3, 4]. Several factors cause capacity fade of Spinel $LiMn_2O_4$, as it had been reported by some investigators [5–11].

(1) Dissolution of Mn^{3+}. At the end of discharge, the concentration of Mn^{3+} arrives at its highest level. Meanwhile, after cycling or storage, the surface of $LiMn_2O_4$ is rich in Mn^{3+}, contrary to the bulk structure. The Mn^{3+} at the surface may disproportionate according to the following reaction:

$$2Mn^{+3}{}_{\text{Solid}} > Mn^{+4}{}_{\text{Solid}} + Mn^{+2}{}_{\text{solutions}}, \quad (1)$$

then, Mn^{2+} ions from this reaction dissolve in the electrolyte solutions.

(2) Jahn Teller effect. At the end of discharge, the Jahn Teller effect happening at first on the surface of some particles may expand into an overall composition of $Li_{[1+\delta]}Mn_2O_4$. Thermodynamically speaking, this system is not really at equilibrium. The phase transition from a cubic into a tetragonal symmetry is a first order process. Even though this kind of distortion is small, it is big enough to destroy the structure to form a tetragonal structure, which is low in symmetry and high in disorder.

(3) In organic solvents, the highly delithiated particles are not stable at the end of discharge; namely, the high oxidation ability of Mn^{4+} will lead to a decomposition of the solvents.

Synthesis approaches of the spinel $LiMn_2O_4$ are various, including solid reaction [12–14], sol-gel reaction [15, 16],

and Pechini process [17]. However, specific capacity of the $LiMn_2O_4$ seems to be independent of the synthesis approaches, which typically is around 120 mAh/g between 3.5 and 4.3 V. Compared to sol-gel and Pechini approaches, in which additional starting materials and synthetic procedures are generally needed for preparation and separation of the targeted Li-Mn precursors, solid reaction is simpler and easier in being handled. Therefore, in this work we selected solid reaction to synthesize spinel $LiMn_2O_4$.

Recent research demonstrated that the importance of surface structural features of electrode materials for their electrochemical performance so, an effective strategy, coating the spinel $LiMn_2O_4$ with organic and inorganic compounds, has been investigated. Jiang et al. [18] coated $LiMn_2O_4$ spinel with 2 wt. %Li-M-PO_4 (M = Co, Ni, Mn) and improved the discharge test by showing the cycling and rate capacities of the spinel $LiMn_2O_4$ cathode materials. $LiFePO_4$ due to its potentially low cost, environmental benignness, and the belief that it could have a major impact in electrochemical energy storage, is the subject of many researches. Also, it can be a good candidate for improving electrochemical properties of conventional cathodes like $LiMn_2O_4$.

In this study, we coated the $LiMn_2O_4$ cathode with nanostructured $LiFePO_4$ layer. The modified $LiMn_2O_4$ can be protected from Mn dissolution, as the $LiFePO_4$ nanostructure is formed on the surface of the spinel $LiMn_2O_4$ cathode. The cycling and rate capacity of $LiMn_2O_4$ cathode materials were significantly enhanced by stabilizing the electrode surface with $LiFePO_4$ nanostructure.

2. Experiment

2.1. Synthesis of $LiMn_2O_4$. Spinel $LiMn_2O_4$ powder was prepared by a solid-state reaction. All starting materials for the synthesis of $LiMn_2O_4$ were purchased from Merck Company. To prepare this spinel, first manganese oxide (II) and lithium hydroxide with molar ratio of 7 : 3 were mechanically mixed. To achieve a more homogenous mixture and lowering calcification time, the mixture was prepared using a planetary mill with higher power, ball to power ratio of 10 : 1, and rotation speed of 200 rpm. Milling was stopped after 15 min and the obtained powder was heated in an electrical tube furnace for 5 hours. The hearting rate of the furnace was $10^\circ C\,min^{-1}$. It must be mentioned that the other parameters of the mill was supposed as constant.

2.2. Synthesis of $LiFePO_4$ Particles and Nanostructure Layers. Sol-gel synthesis is a low temperature, wet chemical approach, which is often used for the preparation of metal oxides or especially thin film. Standard sol-gel synthesis involves the formation of a sol, that is, a stable colloidal suspension of solid particles in a solvent and the gelation of the sol to form a gel consisting of interconnected rigid skeleton with pores made of colloidal particles. The properties of the gel are determined by the particle size and cross linking ratio. The gel can then be dried to form xerogel, which shows reduced volume. To obtain the final products, all liquids need to be removed from the surface of pores by a heat treatment carried out at elevated temperatures [19].

As X-ray diffraction peaks of $LiFePO_4$ thin film layers cannot be detected due to low-weight percentage, first we synthesized phosphate powders by sol gel process to determine optimum synthesis condition. Stoichiometric amounts of lithium phosphate (Li_3PO_4, Aldrich 33,889-3) and phosphoric acid (H_3PO_4, Merck, 100563) were dissolved in 200 mL water by stirring for 60 min. Separately, citrate iron (III)(Merck, S3657400 219) was dissolved in 300 mL of water by stirring for 60 min.The two solutions were mixed together and obtained a transparent gel which was dried at 70°C for 30 h at atmosphere of 99.999% argon. After grinding with a mortar and pestle, the obtained materials were calcined for 1 h. Calcination temperature was measured using thermogravimetry and differential thermal analysis (TG/DTA) result of the dried gel. The heating rate was $10^\circ C\,min^{-1}$. Same sol was used for sol gel dip coating of samples. Three layers of phosphate coat were applied with drawl speed of 10 mm/min, remaining time of 2 min and up speed of 2 mm/min. After each coating step, the sample was dried 70°C for 30 h. Final coated samples were calcined at 670°C for 1 h. Reaction conditions used for preparing different sample of $LiMn_2O_4$ electrodes and $LiFePO_4$ sol were listed in Table 1.

2.3. Structural and Morphological Characterization of Synthesized $LiMn_2O_4$ Powder and $LiFePO_4$ Sol. The thermal decomposition behavior of the gel was examined with a thermogravimetric analyzer (TGA, Perkin Elmer, TAC 7/DX) under N_2 flow. Structural analysis of the obtained products was carried out using an XRD instrument (Philips Expert) with radiation source of Cu-Kα. The surface morphology and energy dispersive spectrometry (EDAX) of the coated particles were taken with a SEM (Philips XL30) microscope. The cyclic voltammogram properties of $LiFePO_4$-coated $LiMn_2O_4$ sample were teted.

2.4. Electrochemical Measurements. Charge and discharge diagrams and cyclic performance were conducted using the AUTOLAB-302 machine. In order to produce $LiMn_2O_4$ cathode with coated $LiFePO_4$, first synthesized $LiMn_2O_4$ as well as carbon black and PTFE binder was mixed together with ratio of 85 : 15 : 5 and was placed in a nickel mesh as current collector. Then, using the dip coating method this mesh was placed in the $LiFePO_4$ sol to contaminate the surface of materials in the mesh. At the end, the mesh was heated at optimum calcination temperature for 1 h in Ar atmosphere. For the negative electrode, the graphite as well as carbon black and PTFE binder was mixed together with ratio of 85 : 15 : 5 and was placed in a nickel mesh as current collector. The used electrolyte was a 1 M solution of $LiClO_4$ in EC: DMC (1 : 1 ratio by volume). Charge/discharge and cyclic voltammetry experiments were carried out in a two-electrode glass cell that was built for this purpose. It must be noted that the battery assemble as well as all electrochemical experiments was performed within the glove box at the presence of Ar atmosphere.

Table 1: Reaction conditions for the preparation of $LiMn_2O_4$ and $LiFePO_4$ sol.

Reaction conditions for the preparation of $LiMn_2O_4$ electrode					Reaction conditions for the preparation of $LiFePO_4$ sol				
Material used	Mn : Li ratio	Sample	Reaction temp (°C)	Reaction time (hrs)	Li precursor	Fe precursor	P precursor	Solvent	Molar ratio
$MnO_2 + LiOH$	7 : 03	A	900	5	$LiOH \cdot H_2O$	$C_6H_5FeO_7 \cdot 2H_2O$	H_3PO_4	Deionized water	1 : 03 : 02
		B	800						
		C	500						
		D	200						

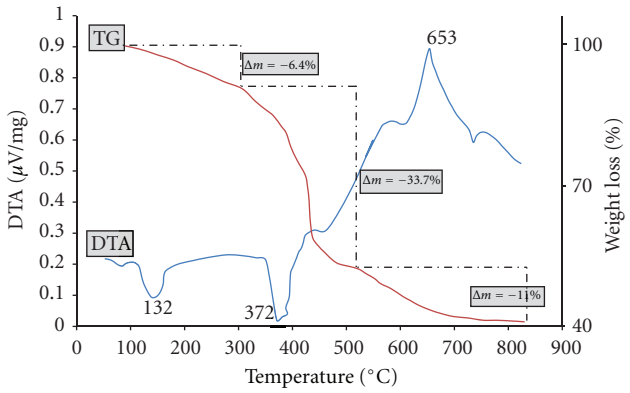

Figure 1: TG and DTA diagrams of gel $LiFePO_4$ at the range of room temperature to 850°C in N_2 atmosphere with heating rate of 10 mL/min.

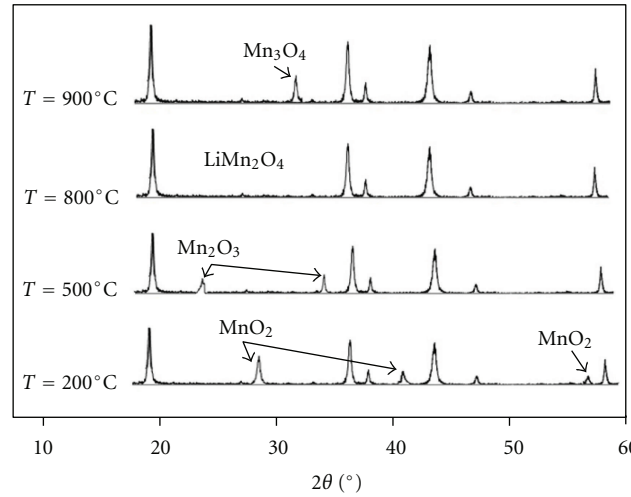

Figure 2: Powder XRD patterns of $LiMn_2O_4$ products after reaction at various temperatures.

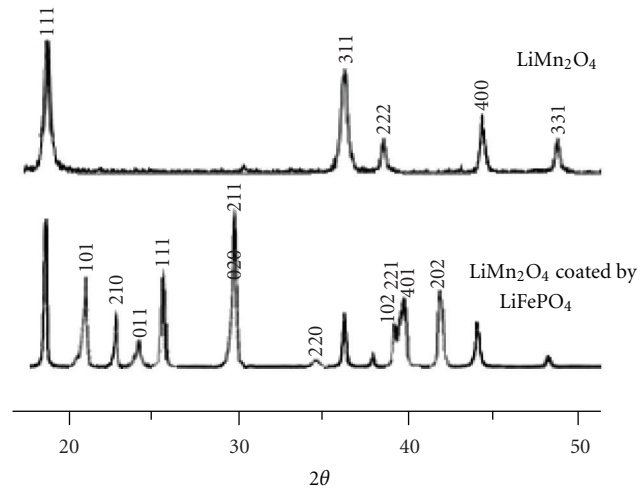

Figure 3: XRD pattern of synthesized products uncoated bare $LiMn_2O_4$, $LiMn_2O_4$ coated with $LiFePO_4$.

3. Results and Discussion

Figure 1 presents DTA and TG diagrams produced for $LiFePO_4$ gel from sole-gel process. The figure exhibits three distinct weight loss zones. At the first step, a weight drop of 6.4% was observed which is due to evaporation of the physically absorbed water and degradation of organic components with the sole. The second loss in within the temperature range of 200 to 500°C, where weight drop is about 33.4% which can be due to release of water during the crystallization as well as pyrolysis of citrate and other organic components. The last weight loss of the given gel will gradually initiate from the temperature of 522°C and continue up to 800°C. The weight drop in this zone is 11% which is due to pyrolysis of remained organic components. All events during the heating of $LiFePO_4$ gel in zones 1 and 2 took place at the temperatures of 132 and 372°C, respectively. These reactions are endothermic, while events occurred in zone 3 are at the temperature of 653°C and are exothermic. So we selected the temperature 670°C as calcination temperature.

Figure 2 shows the progression of the reaction between MnO_2 and LiOH mixed in a 7 : 3 ratio from 200°C to 900°C. As can be seen, the peaks of $LiMn_2O_4$ without any impurities have seen in 800°C. Also, MnO_2 and Mn_2O_3 impurities can be exist at 200°C and 500°C, respectively. The parameters like insufficient temperature and time, decomposition of unreacted MnO_2 can be reasons such impurities, respectively. On the other hand, the XRD patterns at 800°C show clearly the characteristic peaks of the spinel $LiMn_2O_4$ structure, for example, the (111), (311), (222), (400), (331), and (511) peaks. When the heating temperature exceeds 800°C, some characteristic peaks of Mn_3O_4 appear due to excess manganese oxide present in original sample. Given these observations, it could be deduced that with increasing heating temperature, the crystallites of the spinel $LiMn_2O_4$ grow and become ordered and at 800°C a well-ordered spinel structure $LiMn_2O_4$ is produced.

Figure 3 displays XRD pattern for uncoated $LiMn_2O_4$, phosphate components of $LiFePO_4$, and $LiMn_2O_4$ coated by phosphate components of $LiFePO_4$. The lattice constants of bare $LiMn_2O_4$ and modified $LiMn_2O_4$ were calculated from the XRD spectrums which are 0.821 and 0.823 nm, respectively. The modified samples have a larger lattice constant than bare spinel, According to Hu et al. [20], $LiFePO_4$ may form not only a thin layer on the surface of spinel but a solid solution by interacting with spinel. In addition, the decrease in the lattice parameter of the modified sample may be due to substitute iron ion with manganese. The increase of lattice constant can make the crystal structure more stable, leading to the stable cycling performance of $LiFePO_4$-modified $LiMn_2O_4$ during charge/discharge process. Figure 4 shows the surface and cross-section SEM images of $LiFePO_4$ thin film prepared by dip coating sol gel deposited on $LiMn_2O_4$ substrate at 670°C under argon atmosphere with the thickness of about 300 nm. As shown in Figure 4, average grain size of $LiMn_2O_4$ is about 100 nm. Figures 4(b) and 4(c)

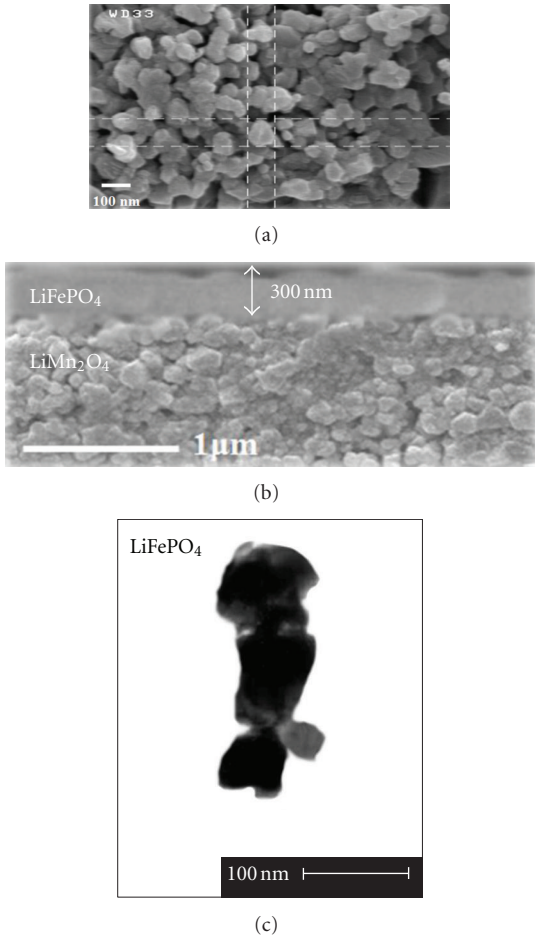

Figure 4: SEM image (a) surface image, (b) cross-section image of $LiFePO_4$ thin film deposited on $LiMn_2O_4$ substrate, (c) TEM image of the $LiFePO_4$ nanoparticle.

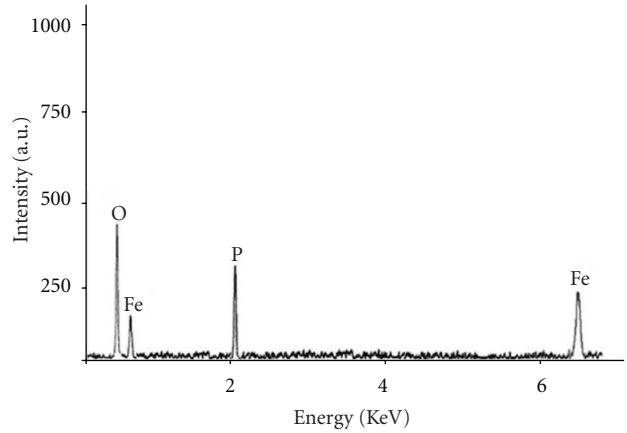

Figure 5: EDX analysis of $LiFePO_4$ nanostructure film.

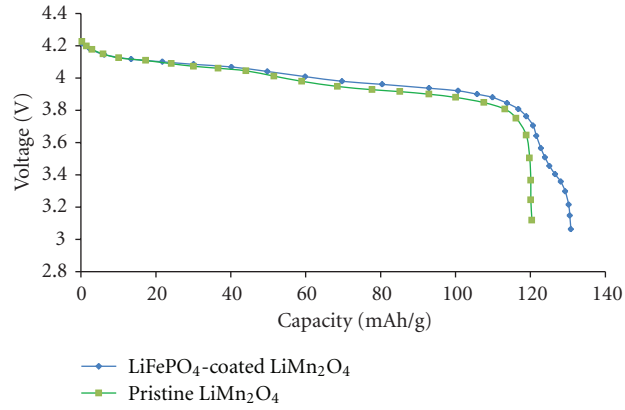

Figure 6: Initial discharge capacities for $LiFePO_4$-coated $LiMn_2O_4$, and pristine $LiMn_2O_4$.

show SEM and TEM images of $LiFePO_4$ coating. As can be seen in Figures 4(b) and 4(c), the thickness of film is about 300 nm. It is interesting to note if the oxide coating is too thin, it may fail to protect the cathode material over long electrochemical cycling; if the oxide coating is too thick, the capacities of the cathode material may be reduced because the oxide coating has higher electronic resistance and higher diffusion resistance for lithium ions [21].

So, based on Figure 4(c) we can conclude that the particle size of $LiFePO_4$ is less than 100 nm, and $LiFePO_4$ film is nanostructure.

Figure 5 shows EDX analysis of the $LiFePO_4$ nanostructure film. Each peak on the spectrum represents a transition with a characteristic energy. Every element has its own "fingerprint" of peaks so we can deduce that it is a represent. The P element can be clearly observed on the surface of modified materials.

The main difference of this study is applying nanostructured $LiFePO_4$ coatings directly on cathode surface instead of surface of cathode particles. Figure 6 shows the initial discharge profile with c-rate performances of the bare $LiMn_2O_4$ and modified by $LiFePO_4$ nanostructure in the voltage range of 3.4–4.3 V. Two plateau features of $LiMn_2O_4$ can be seen in all curves which is the special characterization of lithium manganese dioxide. Figure 7 shows performance of the bare $LiMn_2O_4$ which has been modified by $LiFePO_4$ nanostructure. This cell was tested for 100 cycles at a constant current density of 120 mAh/g (1 C rate: 1 C rate means that the cell has been charged for 1 h upto 4.3 V) and the voltage between 3.0 and 4.3 V. It is clear that surface modification significantly improves the cyclability of $LiMn_2O_4$. Both samples show initial discharge capacity of more than 115 and 125 mAh g^{-1}, respectively. It can be accepted that presence of $LiFePO_4$ phosphate layer leads to a better electrical conductivity of the $LiMn_2O_4$ particles as well as lowering or hindering the additional reactions of cathode materials with the electrolyte. All in all, this not only improves the cyclic capacity of the battery at the higher rates, but also results in higher discharge rates of cathode materials of $LiMn_2O_4$ coated with phosphate layer of $LiFePO_4$.

Figure 8 shows the cyclic voltammogram (CV) of the $LiMn_2O_4$ and $LiFePO_4$-coated $LiMn_2O_4$ electrodes. The voltammetric traces were recorded at a scan rate of 0.05 mV s^{-1}, and lithium served as both the counter and reference electrodes. The bare $LiMn_2O_4$ and LiFePO-coated

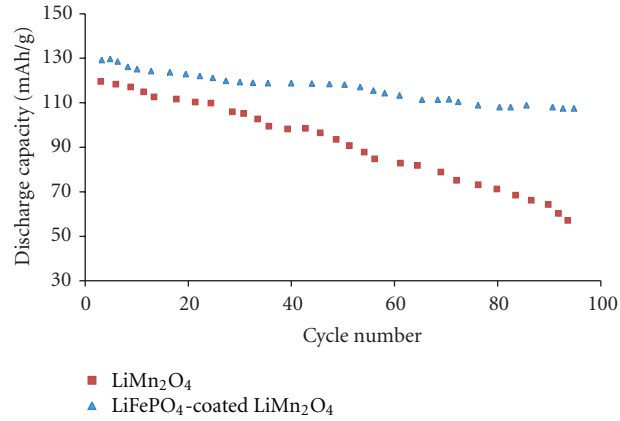

Figure 7: Cycle properties of $LiMn_2O_4$ modified by $LiFePO_4$ nanostructure.

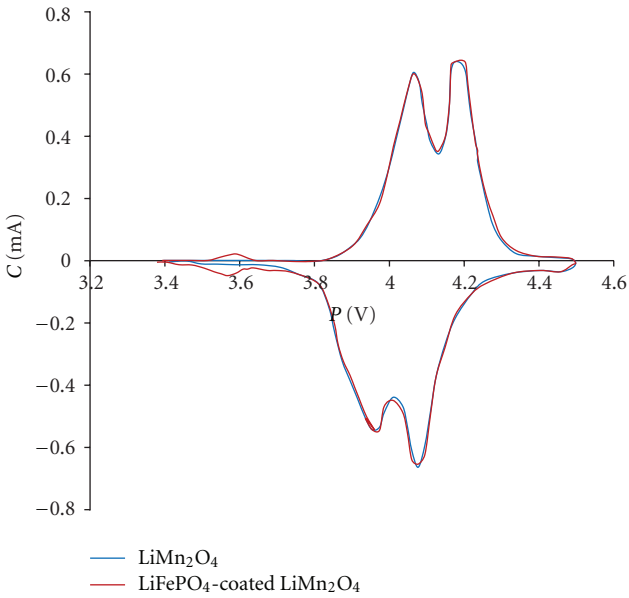

Figure 8: Cyclic voltammograms for bare $LiMn_2O_4$ and $LiFePO_4$-coated $LiMn_2O_4$.

$LiMn_2O_4$ materials exhibited typical voltammograms with different kinetic properties. The CV curves of these samples give two pairs of well-separated reversible oxidation/reduction peaks at around 3.98 and 4.13 V, which are attributed to the splitting of the original Li position in tetrahedral sites (8a). An extra peak at 3.4 V has been observed only for modified one. The presence of the shoulder like appearance at around 3.4 V during the cathodic and anodic sweep corresponded to one of the electrochemical characterizations of $LiFePO_4$ and confirmed the presence of the $LiFePO_4$ layer. [22]. Additionally, the appearance of the dual oxidation and reduction peak corroborated to the coexistence of the $LiMn_2O_4$ phase during cathodic and anodic sweep. From these results, the thin $LiFePO_4$ layer was strongly believed to hamper the Mn dissolution during lithiation, improving the electrochemical performance of $LiFePO_4$-coated $LiMn_2O_4$.

4. Conclusions

Effects on surface modification of the spinel $LiMn_2O_4$ by a $LiFePO_4$ nanostructure as a cathode for Li-ion batteries have been studied as an approach to investigate the electrochemical performance. The results of electrochemical tests showed better capacity retention due to coating layer on the surface of bare $LiMn_2O_4$ material.

References

[1] L. J. Fu, H. Liu, C. Li et al., "Surface modifications of electrode materials for lithium ion batteries," *Solid State Sciences*, vol. 8, no. 2, pp. 113–128, 2006.

[2] C. W. Lee, H. S. Kim, and S. I. Moon, "Effects on surface modification of spinel $LiMn_2O_4$ material for lithium-ion batteries," *Materials Science and Engineering B*, vol. 123, no. 3, pp. 234–237, 2005.

[3] X. Li and Y. Xu, "Enhanced cycling performance of spinel $LiMn_2O_4$ coated with $ZnMn_2O_4$ shell," *Journal of Solid State Electrochemistry*, vol. 12, no. 7-8, pp. 851–855, 2008.

[4] Y. Xia, N. Kumada, and M. Yoshio, "Enhancing the elevated temperature performance of Li/$LiMn_2O_4$ cells by reducing $LiMn_2O_4$ surface area," *Journal of Power Sources*, vol. 90, no. 2, pp. 135–138, 2000.

[5] R. J. Gummow, A. de Kock, and M. M. Thackeray, "Improved capacity retention in rechargeable 4 V lithium/lithium-manganese oxide (spinel) cells," *Solid State Ionics*, vol. 69, no. 1, pp. 59–67, 1994.

[6] J. M. Tarascon, F. Coowar, G. Amatucci, F. K. Shokoohi, and D. Guy-omard, "Synthesis conditions and oxygen stoichiometry effects on Li insertion into the spinel $LiMn_2O_4$," *Journal of The Electrochemical Society*, vol. 141, pp. 1421–1427, 1994.

[7] T. F. Yi, Y. R. Zhu, X. D. Zhu, J. Shu, C. B. Yue, and A. N. Zhou, "A review of recent developments in the surface modification of $LiMn_2O_4$ as cathode material of power lithium-ion battery," *Ionics*, vol. 15, no. 6, pp. 779–784, 2009.

[8] A. M. Kannan and A. Manthiram, "Surface/chemically modified $LiMn_2O_4$ cathodes for lithium-ion batteries," *Electrochemical and Solid-State Letters*, vol. 5, no. 7, pp. A167–A169, 2002.

[9] Y. Ein-Eli, R. C. Urian, W. Wen, and S. Mukerjee, "Low temperature performance of copper/nickel modified $LiMn_2O_4$ spinels," *Electrochimica Acta*, vol. 50, no. 9, pp. 1931–1937, 2005.

[10] D. Jang, Y. Shin, and S. Oh, "Dissolution of spinel oxides and capacity losses in 4 V Li / $Li_xMn_2O_4$ Cells ," *Journal of The Electrochemical Society*, vol. 143, pp. 2204–2211, 1996.

[11] Y. J. Park, J. G. Kim, M. K. Kim, H. G. Kim, H. T. Chung, and Y. Park, "Electrochemical properties of $LiMn_2O_4$ thin films: suggestion of factors for excellent rechargeability," *Journal of Power Sources*, vol. 87, no. 1, pp. 69–77, 2000.

[12] M. M. Thackeray, P. J. Johnson, L. A. De Picciotto, P. G. Bruce, and J. B. Goodenough, "Electrochemical extraction of lithium from $LiMn_2O_4$," *Materials Research Bulletin*, vol. 19, pp. 172–177, 1984.

[13] J. M. Tarascon and D. Guyomard, "Li metal-free rechargeable batteries based on $Li_{1+x}Mn_2O_4$ cathodes ($0 \leq x \leq 1$) and

carbon anodes," *Journal of The Electrochemical Society*, vol. 138, no. 10, pp. 2864–2868, 1991.

[14] Y. Gao and J. R. Dahn, "Synthesis and characterization of $Li_{1+x}Mn_{2-x}O_4$ for Li-ion battery applications," *Journal of The Electrochemical Society*, vol. 143, no. 1, pp. 100–114, 1996.

[15] M. M. Thackeray, "A comment on the structure of thin-film $LiMn_2O_4$ electrodes," *Journal of The Electrochemical Society*, vol. 144, no. 5, pp. L100–L102, 1997.

[16] K. Amine, H. Tukamoto, H. Yasuda, and Y. Fujita, "A new three-volt spinel $Li_{1+x}Mn_{1.5}Ni_{0.5}O_4$ for secondary lithium batteries," *Journal of The Electrochemical Society*, vol. 143, no. 5, pp. 1607–1613, 1996.

[17] W. Liu, G. C. Farrington, F. Chaput, and B. Dunn, "Synthesis and electrochemical studies of spinel phase $LiMn_2O_4$ cathode materials prepared by the pechini process," *Journal of The Electrochemical Society*, vol. 143, no. 3, pp. 879–884, 1996.

[18] Q. L. Jiang, K. Du, Y. B. Cao, Z. D. Peng, G. R. Hu, and Y. X. Liu, "Synthesis and characterization of phosphate-modified $LiMn_2O_4$ cathode materials for Li-ion battery," *Chinese Chemical Letters*, vol. 21, no. 11, pp. 1382–1386, 2010.

[19] O. Toprakci, H. A. K. Toprakci, L. Ji, and X. Zhang, "Fabrication and electrochemical characteristics of $LiFePO_4$ powders for lithium-ion batteries," *Kona Powder and Particle Journal*, vol. 28, pp. 50–73, 2010.

[20] G. R. Hu, X. R. Deng, Z. D. Peng et al., "Comparison of $AlPO_4$- and $Co_3(PO_4)_2$-coated $LiNi_{0.8}Co_{0.2}O_2$ cathode materials for Li-ion battery," *Electrochimica Acta*, vol. 53, no. 5, pp. 2567–2573, 2008.

[21] D. Guan, *Novel surface modifications and new nanostructured titania synthesis for high-performance lithium-ion batteries and solar cells [Ph.D. thesis]*, The Department of Mechanical Engineering, Louisiana State University, 2012.

[22] I. C. Jang, H. H. Lim, S. B. Lee et al., "Preparation of $LiCoPO_4$ and $LiFePO_4$ coated $LiCoPO_4$ materials with improved battery performance," *Journal of Alloys and Compounds*, vol. 497, no. 1-2, pp. 321–324, 2010.